

# Candidate genes responsible for lipid droplets formation during adipogenesis simultaneously affect osteoblastogenesis

Xia Yi<sup>1</sup>, Ping Wu, Ying Gong, Jianyun Liu, Jianjun Xiong, Xiangxin Che, Xiaoyuan Xu

Jiangxi Provincial Key Laboratory of Systems Biomedicine, Jiujiang University, 17 Lufeng Road, Jiujiang 332000, China

## Abstract

**Introduction.** With cellular lipid storage varying, the balance between lipid intake and lipid degradation was a must to keep healthy and determined the level of lipid droplets. Although lipid droplets accumulation had been well demonstrated in adipocytes, gene expression profiling and gene function during adipogenesis and osteoblastogenesis remain unknown.

**Material and methods.** Here, this work profiled gene transcriptional landscapes of lipid droplets formation during adipogenesis from human mesenchymal stem cells (hMSCs) using RNA-Seq technique. By using RNA interference (RNAi) we investigated the function of candidate genes during adipogenesis and osteoblastogenesis using Oil Red/Alizarin Red/alkaline phosphatase (ALPL) staining and qRT-PCR (quantitative real-time PCR).

**Results.** Eleven differentially up-regulated genes associated with lipid droplets formation were identified at 3, 5, 7, 14, 21, and 28 days during adipogenesis. Unexpectedly, *APOB* *per se* inhibiting adipogenesis weakened osteoblastogenesis and *METTL7A* facilitating adipogenesis negligibly inhibited osteoblastogenesis according to the phenotypic characterization of adipocytes and osteoblasts and transcriptional condition of biomarkers through lentivirus transfection assays.

**Conclusions.** The establishment of the gene transcriptional profiling of lipid droplets formation would provide the molecular switches of hMSCs cell fate determination and the study targets for fat metabolic diseases. (*Folia Histochemica et Cytobiologica* 2022, Vol. 60, No. 1, 89–100)

**Key words:** human mesenchymal stem cells (hMSCs); adipogenesis; osteoblastogenesis; *APOB*; *METTL7A*; RNA-seq; siRNA

## Introduction

Thought to be multipotent cells, human mesenchymal stem cells (hMSCs) in adult marrow could be induced to differentiate exclusively into the adipocytes, chondrocytes, or osteocytes [1]. With preadipocytes differentiating into mature adipocytes, the giant and

unilocular lipid droplets grew and expanded during a complex differentiation process of adipogenesis [2]. Mechanistically, lipid droplets formation and adipogenesis were two different events. Interestingly, with the cells maturing sequentially experiencing committed osteo-progenitors, pre-osteoblasts, and terminally differentiated mature osteoblasts, osteoblastogenesis was also associated with lipid droplets accumulation which supplies energy substrates (fatty acids) required by the differentiation process [3]. Clinically, the level of lipid droplets accumulation was determined by the balance between lipid intake and lipid degradation [4].

Lipid droplets, unique multi-functional intracellular organelles that contain a neutral lipid core covered with a phospholipid monolayer membrane

**Corresponding authors:** Xia Yi (yixia@mail.ecust.edu.cn); Jianjun Xiong (jcyx\_xiongjianjun@jju.edu.cn); Xiangxin Che (chexiangxin@jju.edu.cn); Xiaoyuan Xu (xiaoyuan.xu@vip.163.com)

**Correspondence address:** Jiangxi Provincial Key Laboratory of Systems Biomedicine, Jiujiang University, 17 Lufeng Road, Jiujiang 332000, China

[2], are specialized in assembling, storing, and supplying lipids. Classically, neutral lipid droplets predominantly containing triacylglycerols (TAGs) were stored as lipids in adipocytes. Lipid droplets are involved in the regulation of lipid homeostasis by providing the substrates for energy metabolism [5–6], membrane synthesis [7], and production of the essential lipid-derived molecules (lipoproteins, bile salts, or hormones) [8–10]. Till now, the storage, accumulation, and degradation of lipid droplets had been relatively well defined in adipocytes [3, 11–12]. Meanwhile, the contribution of lipid droplets in osteoblasts' formation had also been well established for the utilization of fatty acids to provide ATP [3]. However, little is known about gene transcriptional profiling of lipid droplets formation during adipogenesis and gene function during osteoblastogenesis.

Currently, the best-acknowledged lipid droplets formation during adipogenesis from hMSCs had not been fully elucidated due to the challenging metabolic processes. In our previous study, we tried to establish the relationship between miRNA (microRNA) and lipid droplets formation at 7, 14, 21, 28 days during adipogenesis of hMSCs [13]. Here, this work systematically explored the gene transcriptional profiling of lipid droplets formation during adipogenesis using RNA-Seq technique and confirmed gene function of part of differentially expressed genes (DEGs) of lipid droplets formation during adipogenesis. The establishment of the comprehensive transcriptional profiling for lipid droplets formation during adipogenesis and gene function investigation during adipogenesis and osteoblastogenesis would present molecular switches for controlling hMSCs fate choices and provide the clues for new treatment strategies in fat metabolic diseases.

## Material and methods

**Isolation, identification, and culture of human mesenchymal stem cells.** Identified in the previous study [14], the hMSCs were isolated following the protocols with slight modification [15–16]. In detail, hMSCs were obtained from the cellular fraction of bone marrow after centrifugation at 4°C and 1800 rpm for 20 min. After washing twice with 1 mL of phosphate-buffered saline (PBS, at 4°C and 1400 rpm for 10 min and at 4°C and 1200 rpm for 8 min, respectively), the harvested hMSCs were cultured in 5 mL of a modified Eagle medium ( $\alpha$ -MEM) in 25 cm<sup>2</sup> flasks (Corning Inc., Corning, NY, USA). In a model 3100 series Forma Series II Water Jacket CO<sub>2</sub> incubator (Thermo Fisher Scientific, OH, USA), the hMSCs were cultured in 5.0 mL commercially available hMSCs Basal Medium (Cyagen Biosciences, Inc., Santa Clara, CA, USA) containing 10% FBS (fetal bovine

serum), 2% penicillin-streptomycin, and 1% L-glutamine in 25 cm<sup>2</sup> flasks (Corning Inc., Corning, NY, USA) at 37°C with 5% CO<sub>2</sub> and 95% humidity.

**Differentiation of human mesenchymal stem cells.** Adipogenic differentiation of hMSCs was carried out as previously with slight modifications [17]. Expanded to passage 6, the hMSCs were re-plated at a density of  $5.0 \times 10^4$  cells/cm<sup>2</sup> before adipogenic differentiation. With 80–90% of the final confluence for hMSCs, commercially-available adipogenic cocktails of the hMSCs Basal Medium including 1.0  $\mu$ M dexamethasone, 0.5 mM 3-isobutyl-1-methyl-xanthine (IBMX), and 0.01 mg/mL insulin (SigmaAldrich, St. Louis, MO, USA) were used to stimulate adipogenic differentiation [18]. Adipogenic potential of hMSCs was assessed through Oil Red O (Cyagen Biosciences) staining assays following the protocols [19–20]. Cell morphology and lipid droplets formation in adipocytes were determined using a fluorescence microscope (IX73, Olympus, Tokyo, Japan). The staining assays were carried out in triplicates.

For osteoblastogenic differentiation, the hMSCs were seeded at  $10^8$  cells/cm<sup>2</sup> and cultured to 70% confluence in hMSCs Basal Medium (Cyagen Biosciences, Inc.). Commercial osteoblastogenic differentiation medium supplemented with ascorbic acid, dexamethasone, FBS,  $\beta$ -glycerophosphate, L-glutamine, penicillin, and streptomycin (SigmaAldrich), was used to stimulate osteoblastogenesis every third day. Here, osteoblastogenic potential was assessed via mineralization assays *in vitro* with Alizarin Red staining, alkaline phosphatase (ALPL) staining, and ALPL enzyme activity determination. Calcium-bound Alizarin Red for osteoblasts was eluted after cells were incubated with 100 mM cetylpyridinium chloride for 1 h to quantify the matrix mineralization in a microplate reader (ELx800, Biotek) at the wavelength of 570 nm [21]. The stained osteoblasts were photographed after being washed twice with PBS (pH 8.0). An ALPL staining kit (Jiancheng Bioengineering Institute, Nanjing, China) was used to stain ALPL in a 6-well plate at room temperature (RT) for 10 min after the cells were fixed in cold ethanol for 10 min [22–23]. The photomicrographs were captured with IX73 microscope (Olympus, Tokyo, Japan). The freshly harvested osteoblasts centrifuged at 1000g for 10 min at 4°C were used to determine ALPL enzyme activity with an ALPL assay kit (Jiancheng Bioengineering Institute) after the osteoblasts were lysed on ice using 1.0% Triton-X100 for 40 min. The absorption value of the reaction solution was determined at the wavelength of 520 nm in a microplate reader. All the staining assays were carried out in triplicates.

**RNA-Seq sequencing.** Here, the total RNA was isolated from the adipo-osteoblastogenic cultures at 0, 3, 5, 7, 14, 21, and 28 days using miRNeasy Mini kit (Qiagen, Hilden, Germany) following the manufacturer's instructions. RNA-Seq

**Table 1.** Primers used in this study

Gene	Product	Forward primer (5'-3')	Reverse primer (5'-3')
ACTB	Actin beta	CGAGGACTTTGATTGCACATTG	AGAGAAGTGGGGTGGCTTTTAG
APOB	Apolipoprotein B	TATCAAAAGCCCAGCGTT	GTGCCTACGGCTGGGGAG
LPL	Lipoprotein lipase	GGAAAACAGTCGATCAAGGG	GGCACGATCATCTCTCTCAG
METTL7A	Methyltransferase like 7A	GAGCCCCTAAACATCAAGCAATCT	CTAACACTCGCTTTCAGAGGCCAT
PPARG	Peroxisome proliferator activated receptor gamma	TGCAAGGGTTTCTTCCGG	ATCCCCACTGCAAGGCAT

sequencing performed by NovelBio Bio-Pharm Technology Co., Ltd (Shanghai, China) was separately developed in two batches, one for the samples of 0, 3, 5, and 7 days by HTSeq (Illumina Inc., Towne Centre Drive, San Diego, CA, USA) and the other for the ones of 0, 7, 14, 21, and 28 days by Proton Sequencing (Life Technologies, Gaithersburg, MD, USA).

For HTseq, as in our previous study [24], the freshly isolated RNA with RIN (RNA Integrity Number) > 6.0 was utilized to construct rRNA depletion library using NEBNext® Ultra™ Directional RNA Library Prep kit (New England Biolabs, Ipswich, MA, USA) following the manufacturer's instructions. The sequencing data of the whole transcriptome on Hiseq™ Sequencer was mapped to the human genome after filtering the adaptor sequences including reads with > 5% ambiguous bases and the low-quality reads (more than 20 percent of bases with qualities of < 20). Gene counts of mRNA were calculated using HTSeq [25]. We utilized DESeq to determine the differentially expressed mRNA [26].

Proton Sequencing had been performed in our previous study [17]. The RNA (RIN > 8.0) was used for the construction of cDNA library prepared with Ion Total RNA-Seq Kit v2.0 (Life Technologies Inc., Gaithersburg, MD, USA). cDNA libraries for single-end sequencing were used to process on Proton Sequencing process following the commercially available protocols.

We screened the documented genes associated with lipid droplets formation and their PubMed Unique Identifier (PMID) was listed in Fig. 3c. The visualized transcriptomic heatmap was prepared according to the expression data applicable at least at one sampling point. For data analysis, we set an absolute value of  $\log_2$  ratio  $\geq 2.0$  as the threshold value of the differentially expressed gene (DEGs). Significant DEGs were defined by combining an absolute value of  $\log_2$  ratio  $\geq 2.0$  with FDR (false discovery rate) < 0.001.

**qRT-PCR assays.** To confirm the relative expression level of the target genes, we carried out qRT-PCR (quantitative real-time PCR) on a 7500 Real-Time PCR System (ABI, Foster City, CA, USA) from Bio-Rad Laboratories (Hercules, CA, USA). Oligonucleotide primers used in this study

were synthesized commercially by Generay Biotech Co., Ltd (Shanghai, China) and listed in Table 1. The cDNA synthesis kit (Torobo Co., Osaka, Japan) was used to synthesize the first strand of cDNA. With a SYBR Green Realtime PCR Master Mix (Torobo), PCR amplification profile was as follows: 94°C for 5 min, and then 35 cycles at 94°C for 2 min, 52°C for 30 s, and 72°C for 30 sec. ACTB encoding actin beta was used as the internal control for data acquisition and normalization [27]. qRT-PCR assays were carried out in triplicates.

**Cell transfection.** To determine the function of lipid droplets formation genes, we separately knocked down *APOB* and *METTL7A* to investigate the gene function during adipogenesis and osteoblastogenesis through RNA interference (RNAi). The sequences, 5' — cgGAACTATCAACTCTACAAA — 3' for *APOB* (NM\_000384.3), 5' — atAGTGTGAGCTGGCAGTTAA — 3' for *METTL7A* (NM\_014033), and 5' - TTCTCCGAACGTGTCACGT - 3' for the negative control, synthesized commercially by Genechem Co., Ltd (Shanghai, China), were constructed in pGV493-*GFP* vector to establish the expressing plasmid for RNAi following the standard sub-cloning procedures [28, 29]. For cell transfection assays, 4  $\mu$ L *APOB*-siRNA and 2.5  $\mu$ L *METTL7A*-siRNA lentivirus ( $2 \times 10^8$  infectious units/mL; MOI, multiplicity of infection = 10) were performed at 20% confluence (approximately  $3.2 \times 10^5$  cells) of hMSCs using HitransG Transfection Reagent P (Genechem Inc., Shanghai, China) at 37°C following the manufacturer's instruction. Fluorescence intensity of GFP (green fluorescent protein) was determined using a fluorescence microscope (IX73, Olympus, Tokyo, Japan) after approximately 72 h of transfection. Adipogenic and osteoblastogenic differentiation assays were carried out at 72 h and 12 h after transfection, respectively.

**Statistical analyses.** Using SigmaPlot version 14 software (Systat Software, Inc., San Jose, CA, USA), the significant difference ( $p < 0.001$ ) was derived from Student's t-test (or the Mann-Whitney Rank Sum Test) wherever an appropriate depending normality test. A p-value of less than 0.05 ( $p < 0.05$ ) was defined statistically significant with  $n = 3$  for each group.

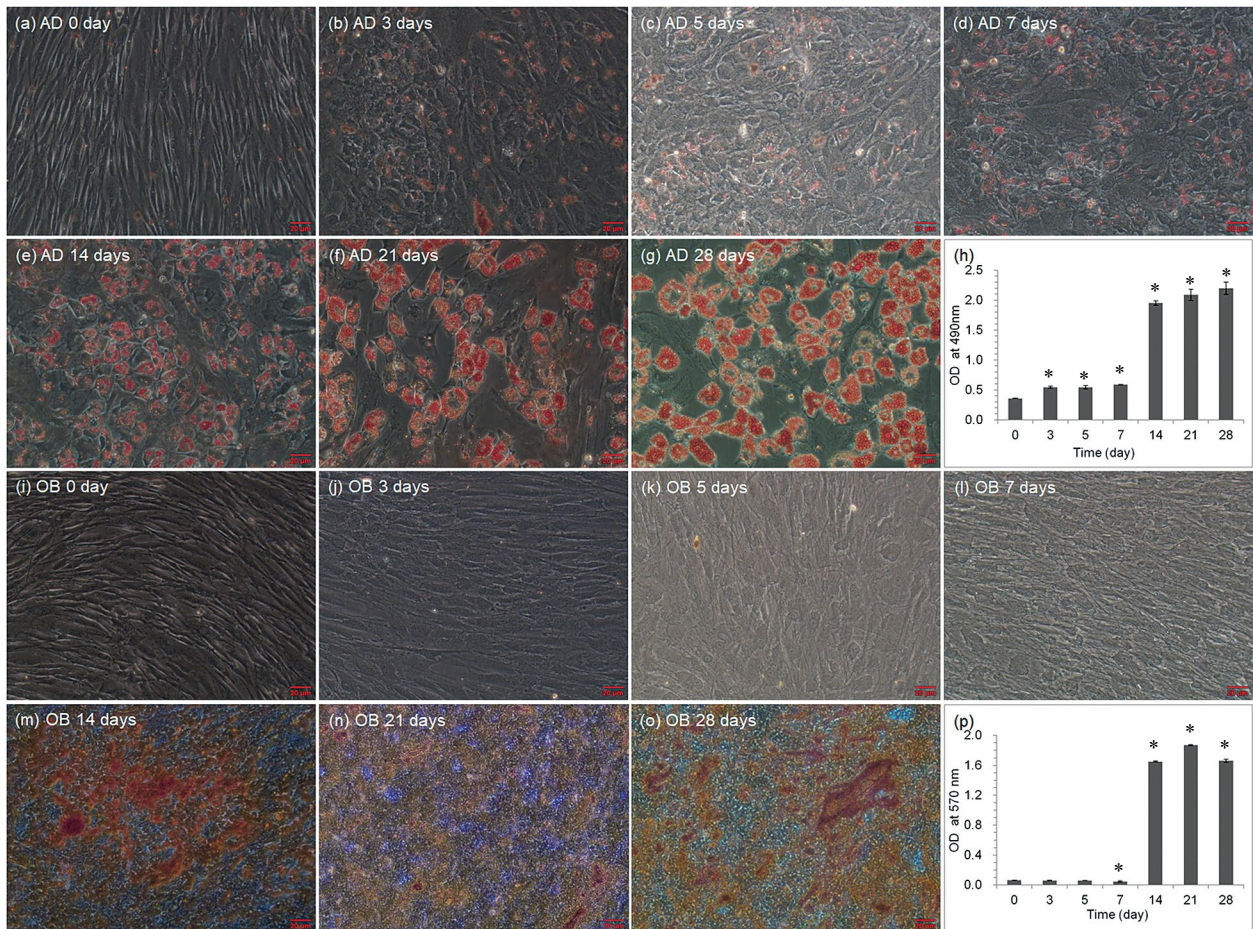


**Figure 1.** Adipo- and osteoblastogenic potential of hMSCs. Microphotographs (a–g) and (i–o) separately indicate adipogenesis (AD) by staining the differentiating hMSCs with Oil Red O, and osteoblastogenesis (OB) by staining with Alizarin Red O. (h) and (p) indicated the quantification of light absorption by lipid droplets and the mineralized bone matrix, respectively, as described in Methods. Scale bars: 20  $\mu$ m. Bars and whiskers indicate means  $\pm$  SD (standard deviation). \* $p < 0.05$ ,  $n = 3$  for each group. OD — optical density.

## Results

### *Adipo-osteoblastogenic potential of the hMSCs*

Adipogenic potential of hMSCs was assessed through lipid droplets staining using Oil Red O (Fig. 1). Compared with the undifferentiated control group at 0 day, lipid droplets were first visible at 3 days, and the number and size of lipid droplets slowly increased with the cell culture time prolonged from 0 days to 7 days (Fig. 1a–d). Lipid droplets' growth and expansion were more and more apparent from 14 to 28 days (Fig. 1e–g). The maximum amount of lipid droplets formation appeared from 14 to 28 days during adipogenesis (Fig. 1h).

For osteoblastogenesis, we visualized the morphological changes of the cultured cells that became more rounded and cobblestone-like shape on the 3rd day of culture. A lower fraction of osteoblasts was stained

by Alizarin Red from 3 to 7 days, but an increased secretion of mineralized bone matrix appeared from 14 to 28 days (Fig. 1i–o). As Figs. 1h and 1p showed, although the quantification of lipid droplets formation from 3 to 7 days during adipogenesis was more than that of matrix mineralization accumulation during adipogenesis and adipo-osteoblastogenesis, the maximum amount appeared from 14 to 28 days during the two differentiated processes. Herein, these results indicated that the hMSCs differentiated along adipogenesis and osteoblastogenesis, respectively.

### *Gene expression profiling of lipid droplets formation*

RNA-Seq's were performed to investigate gene expression profiling at 3, 5, 7, 14, 21, and 28 days during adipogenesis from hMSCs. As Figs. 2a and 2b showed that the gene expression level of adipogenic and os-

teoblastogenic biomarkers corresponded with that of the classic documented ones [30], and thus indicated the deep-sequencing data were authentic. According to statistical analysis, the significant biomarker genes included *ADIPOQ*, *CEBPA*, *FABP4*, *FASN*, *ID3*, *LPL*, *PPARG*, and *SREBF1* for adipogenesis and *ALPL*, *SPP1*, and *TWIST* for osteoblastogenesis.

Among seventy-nine published genes of lipid droplets formation process listed in Fig. 2c, fourteen up- and one down-regulated DEGs were identified at 3, 5, and 7 days of culture by HTSeq, and eleven differentially up-regulated genes were screened at 7, 14, 21, and 28 days of culturing hMSCs by Proton Sequencing. Eleven genes (*ACACB*, *ACSL1*, *APOB*, *CES1*, *CIDEA*, *G0S2*, *LIPE*, *METTL7A*, *PLIN1*, *PLIN4*, and *STOM*) were differentially up-regulated at 3, 5, 7, 14, 21, and 28 days during adipogenesis (Fig. 2c), and thus suggesting that the target genes were responsible for adipogenic differentiation.

#### Candidate genes simultaneously affected adipo-osteoblastogenesis

To confirm the gene function of the DEGs associated with lipid droplets formation, both *APOB* and *METTL7A* were subjected to additional validation experiments. Fluorescence microscopy assays revealed that the hMSCs were transfected successfully using the negative, *APOB*-siRNA, and *METTL7A*-siRNA lentiviruses (Fig. 3A). Moreover, more than 90% and 20% of transfection efficiency was the criterion of adipogenic and osteoblastogenic differentiation, respectively (Fig. 3B). It showed that *APOB* knockdown promoted adipogenesis at 3 and 7 days, as indicated by changes at the mRNA levels (Fig. 3C) and accumulation of lipid droplets (Fig. 3D). *METTL7A* knockdown weakened adipogenesis for the abasement of adipogenic biomarkers at gene transcriptional level and decreased lipid droplets accumulation (Fig. 3A–3C). Thus, we showed that *APOB* and *METTL7A* inhibited and promoted adipogenesis, respectively. Among the eleven screened genes, *APOB* and *METTL7A* were the two of the randomly confirmed candidates for lipid droplets formation during adipogenesis, thus suggesting the other candidates listed in Fig. 2C would be of the same importance for adipogenesis.

For the purpose of verification of the role played by *APOB* and *METTL7A* during osteoblastogenesis, we also profiled transcriptional landscapes of lipid droplets formation genes during osteoblastogenesis. Fig. 2C illustrates that *APOB* was differentially up-regulated 16.48, 15.84, 16.29, 12.13, 11.98, 12.37, and 10.91 folds at 3, 5, 7, 7, 14, 21, and 28 days during osteoblastogenesis, respectively, and *METTL7A* was also up-regulated by 1.46, 1.54, 1.73, 1.04, 1.12,

1.90, and 2.08 folds during osteoblastogenesis. With *APOB* and *METTL7A* knocked down, the expression of *ALPL* was just increased separately at 7 days and 3 days during osteoblastogenesis (Fig. 3C), and the mRNA level of *RUNX2* was promoted at 3, 7, and 14 days during osteoblastogenesis.

Mineral deposits determination using Alizarin red staining demonstrated that *APOB* knockdown led to an increase at 7 and 14 days, and the latter was improved a little more (Fig. 3E). It showed that a negligible increase of matrix mineralization occurred at 3 and 14 days after knocking down *METTL7A* (Fig. 3E). Compared with the control, enzyme activity of *ALPL* was increased in cells with *APOB* and *METTL7A* silencing (Fig. 3F). Thus, the lipid droplet formation-related candidate genes during adipogenesis would play also simultaneously critical roles in osteoblastogenesis with partly confirmed involvement of *APOB* and *METTL7A* genes.

#### Discussion

Extracellular matrix (ECM) of MSCs not only determines MSC lineage differentiation *via* multiple mechanisms [30] but also predominantly contributes to MSC heterogeneity [31]. As complex and dynamic organelles, lipid droplets had been well documented in many cell types particularly in disease states and important biological processes like autophagy [32–33]. Here, to our best knowledge, we are the first to uncover the contribution of lipid droplets formation genes to adipogenesis and osteoblastogenesis using RNA-seq technique.

As we know, lipid droplets formation underwent the formation of an oil lens, budding and nascent lipid droplets formation, and growth and expansion of lipid droplets [2]. Lipid droplets grew and expanded with the culture time prolonged from 3 to 28 days during adipogenesis. In the present study, changes in lipid droplets formation were just seen on days 3 and 7 but not day 14 during adipogenesis. The early stage of differentiation was an important process for adipogenesis of hMSCs. *PPARG* (peroxisome proliferation activated receptor gamma) and *CEBPA* (CCAAT enhancer-binding protein alpha) were considered to regulate the early stage of adipogenesis, while *ADIPOQ* (adiponectin, C1Q and collagen domain containing) and *FASN* (fatty acid synthase) were responsible for the mature adipocyte formation [32], and thus the indicated days 3 and 7 of sampling time point were the vital stages of lipid droplets formation.

Here, we used adipogenic cocktails including dexamethasone, IBMX, and insulin, to stimulate our adipogenesis from hMSCs. Although adipocytes

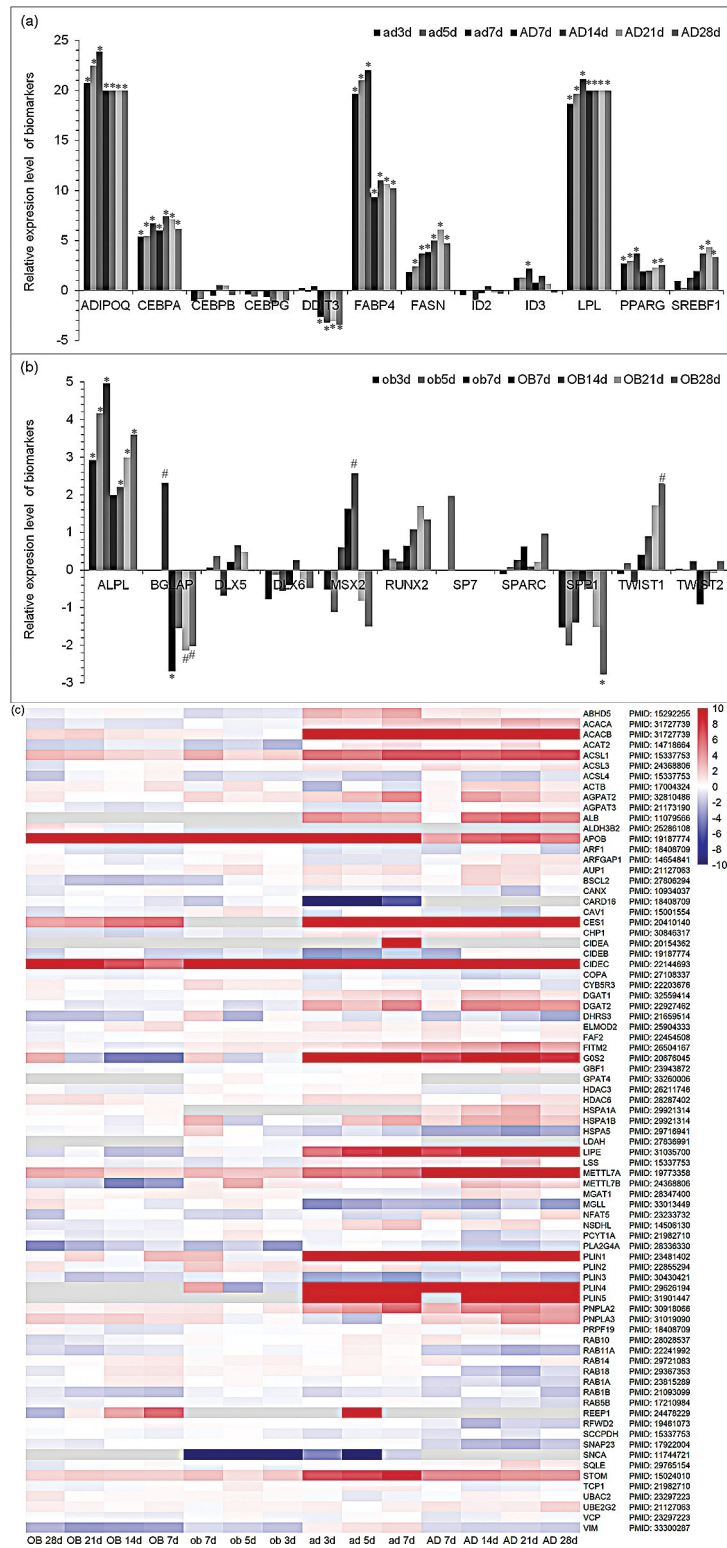
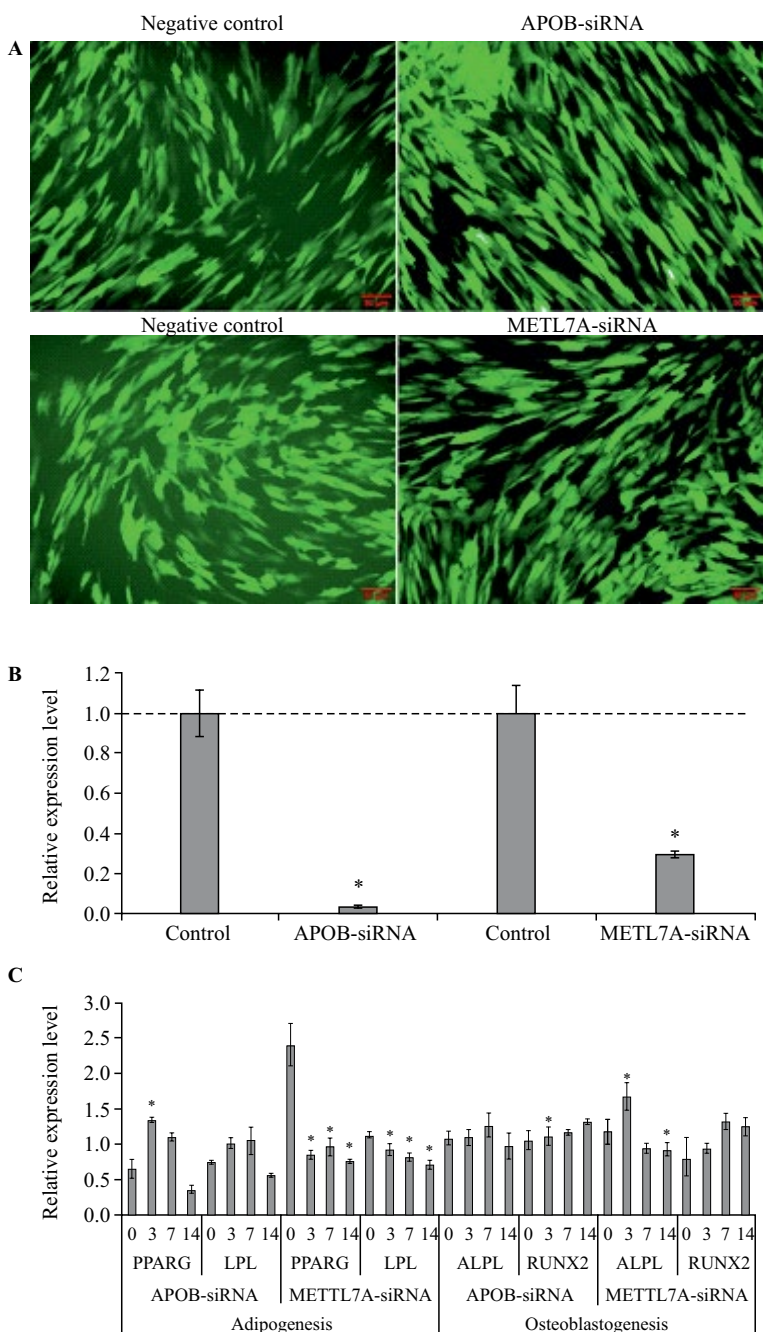


**Figure 2.** Gene expression profiling of lipid droplets formation during adipo- and osteoblastogenesis of hMSCs. **A.** Expression level of adipogenic biomarkers from RNA-Seq sequencing data. **B.** Expression level of osteoblastogenic biomarkers from RNA-Seq sequencing data; **C.** Heat-map of lipid droplets formation genes for adipogenesis according to RNA-Seq sequencing. The color scale in the upper right corner represents the expression level of the up- and down-regulated genes. The symbols # and \* indicate differentially expressed genes and significantly expressed genes (FDR < 0.001), respectively. The upper-case AD indicates RNA-Seq sequencing by Proton Sequencing at 7, 14, 21, and 28 d, and the lower-case ad indicate RNA-Seq sequencing by HTSeq at 3, 5, and 7 d. NA — not applicable. PMID (pubMed unique identifier) indicates the gene resource of lipid droplets formation. Eleven genes, including *ACACB*, *ACSL1*, *APOB*, *CES1*, *CIDEA*, *GOS2*, *LIPE*, *METTL7A*, *PLIN1*, *PLIN4*, and *STOM* were differentially expressed at 3, 5, 7, 14, 21, and 28 days during adipogenesis.

increased in size (hypertrophy) and number (hyperplasia) for adipose tissue expansion [34], they could not grow and accumulate lipids without restriction but divided into two or more adipocytes after reaching a certain size. It showed that cellular growth of the differentiating pre-adipocytes was stopped after reaching a certain confluence under standard culture conditions. But, when a hormonal cocktail was added, adipocytes were further divided before differentiation program termination and development into mature adipocytes.

In the present work, the eleven identified DEGs during adipogenesis included *ACACB*, *ACSL1*,

*APOB*, *CES1*, *CIDEA*, *G0S2*, *LIPE*, *METTL7A*, *PLIN1*, *PLIN4*, and *STOM*. *ACACB* (acetyl-CoA carboxylase beta) is preferentially related with fatty acid oxidation [35–36]. *ACSL1* encoding long-chain acyl-CoA synthetase 1 belongs to the family of acyl-CoA synthetases and plays an important role in lipid metabolism [37]. As macromolecular micelles of lipid and protein and a specialized transport vehicle for hydrophobic lipids [38], *APOB* (apolipoprotein B) is closely related to lipid droplets biogenesis [15, 39–40] being involved with atherosclerotic disease [41], atherogenic risk [42–44], and common dyslipoproteinemia [45–48]. *CES1* encoding carboxylesterase 1 is an



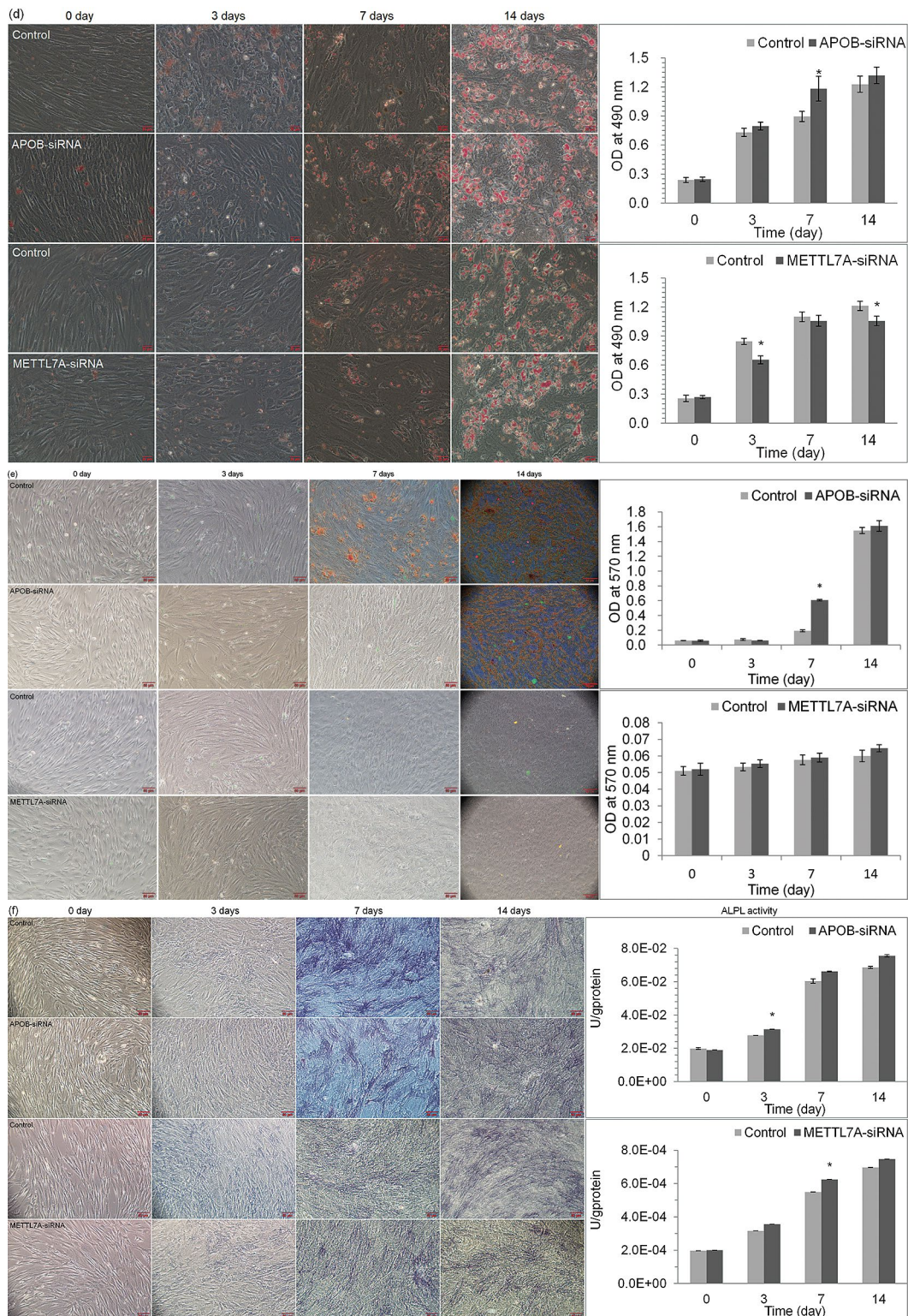


**Figure 3.** *APOB* and *METTL7A* regulate adipo-osteoblastogenesis from hMSCs. (a) Fluorescence intensity of GFP (green fluorescent protein) indicating transfection efficiency after silencing by RNA interference (RNAi). Scale bar: 50  $\mu$ m. (b) The relative expression level of *APOB* and *METTL7A* after RNAi silencing. (c) The relative expression level of the genes encoding biomarkers after silencing of *APOB* and *METTL7A* genes, such as *PPARG* and *LPL* for adipogenesis, and *ALPL* and *RUNX2* for osteoblastogenesis. (d) Evaluation of adipogenic potential by Oil Red O staining after silencing of *APOB* and *METTL7A* genes. (e) Evaluation of osteoblastogenic potential by Alizarin Red staining after silencing of *APOB* and *METTL7A* genes. (f) Alkaline phosphatase (ALPL) staining and enzyme's activity in cell lysates after silencing of *APOB* and *METTL7A* genes were determined as described in Methods. Scale bar: 20  $\mu$ m. Bars and error bars at (e–f) represent mean  $\pm$  SD. \* $p < 0.05$  ( $n = 3$ ).

essential NF- $\kappa$ B-regulated lipase [49]. *CIDEA* (cell death inducing DFFA like effector c) promotes lipid droplets formation in adipocytes [50]. *G0S2* (G0/G1 switch 2) is involved in adipogenic differentiation of preadipocytes for its mRNA level up-regulated and attenuated ATGL-mediated lipolysis [51–52]. *LIPE* (lipase E, hormone-sensitive type) converts cholesterol esters from lipid droplets to free cholesterol [53]. As one of the targets for the non-coding RNA [15], *METTL7A* (methyltransferase like 7A, also known as *AAM-B* or *AAMB*) protein is located in lipid droplets surface as a signaling factor and is tightly related with lipid droplets formation [54–57]. Belonging to the classical PAT family (perilipin (perilipin 1), adipophilin (perilipin 2), and TIP47 (perilipin 3)) of lipid droplet proteins, PLIN1 (perilipin 1) also known as adipose differentiation-related protein (ADRP) is localized at the surface of lipid droplets and regulates triglyceride storage and hydrolysis in adipocytes [58]. PLIN4 (perilipin 4) could cover a large lipid droplet surface and could act as a substitute for phospholipids [59]. STOM (stomatatin) was targeted to cytoplasmic lipid bodies [60]. Our omics data affirmatively provided the molecular evidence for the involvement of lipid droplet formation-related genes in response to adipogenic differentiation of bone marrow-derived hMSCs.

The osteoblast progenitor cells and their committed osteoprogenitor cells always use lipid droplets as an endogenous source of fatty acids [3]. In this work, when the gene function of *APOB* and *METTL7A* was confirmed, we tried to find out the contribution of genes involved in lipid droplets formation to osteoblastogenesis. An intriguing relationship always existed between fracture risk, bone mass, and marrow adiposity [59–60]. hMSCs pre-committed to one mesenchyme cell lineage could transdifferentiate to other cell types in response to inductive extracellular cues [63–67]. Cell dedifferentiation and transdifferentiation were important for the regulation of lineage commitment. The multilineage differentiation potential of hMSCs is significant for tissue regeneration in clinical utility. Control of cell-fate decisions for hMSCs is tightly regulated by genes [68], growth factors/cytokines and their cognate receptors [69], and melatonin [70]. In this work, we provided more cues for the contribution of *APOB* and *METTL7A* to the balance of hMSCs differentiation.

The present study has its limitation. First, for sequencing data, RNA-Seq was separately carried out in two batches using HTSeq and Proton Sequencing of two different sequencing platforms. So, the sequencing data of two points at 7 days were not completely consistent, although the expression trend

of most genes was almost consistent. Second, for hMSCs culture, the medium and operation technology directly affected the gene transcription and protein translation. Here, although we cultured the hMSCs for adipogenesis and osteoblastogenesis assays together, we assessed adipogenic potential (qPCR and Oil Red O staining for lipid droplets formation) and osteoblastogenic potential (qPCR, Alizarin Red staining for mineralization, ALPL staining, and ALPL enzyme activity determination) in different batches for the numerous experiments. Third, it is well established that *RUNX2* is the classic biomarker for osteoblastogenesis study [71]. Accidentally, we found the expression level of *RUNX2* was not differentially expressed for all sampling time points. Perhaps, the secreted calcium largely affected RNA harvest and then the expression of osteoblastogenic biomarkers. Therefore, the further clue for the contribution of lipid droplets formation genes to adipogenesis and osteoblastogenesis would be put forward for the balance regulation of hMSCs differentiation.

In summary, this study represented one of the first general reports of the gene transcriptional profiling of lipid droplets formation during adipogenesis of differentiating hMSCs. Interestingly, the DEGs would be the potential molecular switches of hMSCs cell fate determination with *APOB* and *METTL7A* confirmed. Establishing the gene transcriptional profiling of lipid droplets formation might also lead to a novel approach to study metabolic bone diseases.

## Funding

This research was supported by the National Natural Science Foundation of China (81760167/82160174/81860165), Jiangxi Provincial Natural Science Foundation (20202ACB206003).

## Author contributions

XY designed the experiment, partially analyzed the RNA-Seq data and visualized data presentation, performed qRT-PCR experiment, and prepared the manuscript. XY, PW, and YG performed cell culture. XY and JYL carried out western blot experiments. XY, JJX, XXC, and XYX were in charge of the overall project. All authors read and approved the final manuscript.

## Ethics approval

With written informed consent signed, a 21-year-old non-osteoporotic healthy male volunteer was recruited by Affiliated Hospital of Jiujiang University

in this study. The study is compliant with all relevant ethical regulations approved by the Medical Ethics Committee of Jiujiang University (Approved ID: 1-2013, February 20, 2013).

## Data availability statements

RNA-Seq sequence data were deposited in the GEO database at NCBI with accession numbers GSE174794 and GSE175624.

## Conflict of interests

The authors declare that there are no competing interests associated with the manuscript.

## References

- Pittenger MF, Mackay AM, Beck SC, et al. Multilineage potential of adult human mesenchymal stem cells. *Science*. 1999; 284(5411): 143–147, doi: [10.1126/science.284.5411.143](https://doi.org/10.1126/science.284.5411.143), indexed in Pubmed: [10102814](https://pubmed.ncbi.nlm.nih.gov/10102814/).
- Walther TC, Chung J, Farese RV. Lipid droplet biogenesis. *Annu Rev Cell Dev Biol*. 2017; 33: 491–510, doi: [10.1146/annurev-cellbio-100616-060608](https://doi.org/10.1146/annurev-cellbio-100616-060608), indexed in Pubmed: [28793795](https://pubmed.ncbi.nlm.nih.gov/28793795/).
- Rendina-Ruedy E, Guntur AR, Rosen CJ. Intracellular lipid droplets support osteoblast function. *Adipocyte*. 2017; 6(3): 250–258, doi: [10.1080/21623945.2017.1356505](https://doi.org/10.1080/21623945.2017.1356505), indexed in Pubmed: [28792783](https://pubmed.ncbi.nlm.nih.gov/28792783/).
- Krahmer N, Farese RV, Walther TC. Balancing the fat: lipid droplets and human disease. *EMBO Mol Med*. 2013; 5(7): 973–983, doi: [10.1002/emmm.201100671](https://doi.org/10.1002/emmm.201100671), indexed in Pubmed: [23740690](https://pubmed.ncbi.nlm.nih.gov/23740690/).
- Li L, Zhang H, Yao Y, et al. (-)-Hydroxycitric acid suppresses lipid droplet accumulation and accelerates energy metabolism via activation of the adiponectin-AMPK signaling pathway in broiler chickens. *J Agric Food Chem*. 2019; 67(11): 3188–3197, doi: [10.1021/acs.jafc.8b07287](https://doi.org/10.1021/acs.jafc.8b07287), indexed in Pubmed: [30827101](https://pubmed.ncbi.nlm.nih.gov/30827101/).
- Wang M, Yi X. Bulging and budding of lipid droplets from symmetric and asymmetric membranes: competition between membrane elastic energy and interfacial energy. *Soft Matter*. 2021; 17(21): 5319–5328, doi: [10.1039/d1sm00245g](https://doi.org/10.1039/d1sm00245g), indexed in Pubmed: [33881134](https://pubmed.ncbi.nlm.nih.gov/33881134/).
- Romanauska A, Köhler A. Reprogrammed lipid metabolism protects inner nuclear membrane against unsaturated fat. *Dev Cell*. 2021; 56(18): 2562–2578.e3, doi: [10.1016/j.devcel.2021.07.018](https://doi.org/10.1016/j.devcel.2021.07.018), indexed in Pubmed: [34407429](https://pubmed.ncbi.nlm.nih.gov/34407429/).
- Zheng XY, Yu BL, Xie YF, et al. Apolipoprotein A5 regulates intracellular triglyceride metabolism in adipocytes. *Mol Med Rep*. 2017; 16(5): 6771–6779, doi: [10.3892/mmr.2017.7461](https://doi.org/10.3892/mmr.2017.7461), indexed in Pubmed: [28901468](https://pubmed.ncbi.nlm.nih.gov/28901468/).
- Casado ME, Huerta L, Marcos-Díaz A, et al. Hormone-sensitive lipase deficiency affects the expression of SR-BI, LDLr, and ABCA1 receptors/transporters involved in cellular cholesterol uptake and efflux and disturbs fertility in mouse testis. *Biochim Biophys Acta Mol Cell Biol Lipids*. 2021; 1866(12): 159043, doi: [10.1016/j.bbalip.2021.159043](https://doi.org/10.1016/j.bbalip.2021.159043), indexed in Pubmed: [34461308](https://pubmed.ncbi.nlm.nih.gov/34461308/).
- Pabois O, Ziolk RM, Lorenz CD, et al. Morphology of bile salts micelles and mixed micelles with lipolysis products, from scattering techniques and atomistic simulations. *J Colloid Interface Sci*. 2021; 587: 522–537, doi: [10.1016/j.jcis.2020.10.101](https://doi.org/10.1016/j.jcis.2020.10.101), indexed in Pubmed: [33189321](https://pubmed.ncbi.nlm.nih.gov/33189321/).
- Zahradka P, Neumann S, Aukema HM, et al. Adipocyte lipid storage and adipokine production are modulated by lipoxygenase-derived oxylipins generated from 18-carbon fatty acids. *Int J Biochem Cell Biol*. 2017; 88: 23–30, doi: [10.1016/j.biocel.2017.04.009](https://doi.org/10.1016/j.biocel.2017.04.009), indexed in Pubmed: [28465089](https://pubmed.ncbi.nlm.nih.gov/28465089/).
- Heid H, Zimmelmann R, Dörflinger Y, et al. Formation and degradation of lipid droplets in human adipocytes and the expression of aldehyde oxidase (AOX). *Cell Tissue Res*. 2020; 379(1): 45–62, doi: [10.1007/s00441-019-03152-1](https://doi.org/10.1007/s00441-019-03152-1), indexed in Pubmed: [31858241](https://pubmed.ncbi.nlm.nih.gov/31858241/).
- Yi X, Liu J, Wu P, et al. The key microRNA on lipid droplet formation during adipogenesis from human mesenchymal stem cells. *J Cell Physiol*. 2020; 235(1): 328–338, doi: [10.1002/jcp.28972](https://doi.org/10.1002/jcp.28972), indexed in Pubmed: [31210354](https://pubmed.ncbi.nlm.nih.gov/31210354/).
- Xu X, Li X, Yan R, et al. Gene expression profiling of human bone marrow-derived mesenchymal stem cells during adipogenesis. *Folia Histochem Cytobiol*. 2016; 54(1): 14–24, doi: [10.5603/FHC.a2016.0003](https://doi.org/10.5603/FHC.a2016.0003), indexed in Pubmed: [27044590](https://pubmed.ncbi.nlm.nih.gov/27044590/).
- Yi X, Wu P, Liu J, et al. Identification of the potential key genes for adipogenesis from human mesenchymal stem cells by RNA-Seq. *J Cell Physiol*. 2019; 234(11): 20217–20227, doi: [10.1002/jcp.28621](https://doi.org/10.1002/jcp.28621), indexed in Pubmed: [30989650](https://pubmed.ncbi.nlm.nih.gov/30989650/).
- Casado-Díaz A, Santiago-Mora R, Jiménez R, et al. Cryopreserved human bone marrow mononuclear cells as a source of mesenchymal stromal cells: application in osteoporosis research. *Cytotherapy*. 2008; 10(5): 460–468, doi: [10.1080/14653240802192644](https://doi.org/10.1080/14653240802192644), indexed in Pubmed: [18608349](https://pubmed.ncbi.nlm.nih.gov/18608349/).
- Nakamura T, Shiojima S, Hirai Y, et al. Temporal gene expression changes during adipogenesis in human mesenchymal stem cells. *Biochem Biophys Res Commun*. 2003; 303(1): 306–312, doi: [10.1016/s0006-291x\(03\)00325-5](https://doi.org/10.1016/s0006-291x(03)00325-5), indexed in Pubmed: [12646203](https://pubmed.ncbi.nlm.nih.gov/12646203/).
- Wang YL, Lin SP, Hsieh PCH, et al. Concomitant beige adipocyte differentiation upon induction of mesenchymal stem cells into brown adipocytes. *Biochem Biophys Res Commun*. 2016; 478(2): 689–695, doi: [10.1016/j.bbrc.2016.08.008](https://doi.org/10.1016/j.bbrc.2016.08.008), indexed in Pubmed: [27498007](https://pubmed.ncbi.nlm.nih.gov/27498007/).
- Ross SE, Hemati N, Longo KA, et al. Inhibition of adipogenesis by Wnt signaling. *Science*. 2000; 289(5481): 950–953, doi: [10.1126/science.289.5481.950](https://doi.org/10.1126/science.289.5481.950), indexed in Pubmed: [10937998](https://pubmed.ncbi.nlm.nih.gov/10937998/).
- Donzelli E, Lucchini C, Ballarini E, et al. ERK1 and ERK2 are involved in recruitment and maturation of human mesenchymal stem cells induced to adipogenic differentiation. *J Mol Cell Biol*. 2011; 3(2): 123–131, doi: [10.1093/jmcb/mjq050](https://doi.org/10.1093/jmcb/mjq050), indexed in Pubmed: [21278199](https://pubmed.ncbi.nlm.nih.gov/21278199/).
- Chen J, Liu M, Luo X, et al. Exosomal miRNA-486-5p derived from rheumatoid arthritis fibroblast-like synoviocytes induces osteoblast differentiation through the Tob1/BMP/Smad pathway. *Biomater Sci*. 2020; 8(12): 3430–3442, doi: [10.1039/c9bm01761e](https://doi.org/10.1039/c9bm01761e), indexed in Pubmed: [32406432](https://pubmed.ncbi.nlm.nih.gov/32406432/).
- Shi Y, Chen J, Karner CM, et al. Hedgehog signaling activates a positive feedback mechanism involving insulin-like growth factors to induce osteoblast differentiation. *Proc Natl Acad Sci U S A*. 2015; 112(15): 4678–4683, doi: [10.1073/pnas.1508257112](https://doi.org/10.1073/pnas.1508257112), indexed in Pubmed: [25825734](https://pubmed.ncbi.nlm.nih.gov/25825734/).
- Shi Yu, Fu Y, Tong W, et al. Uniaxial mechanical tension promoted osteogenic differentiation of rat tendon-derived stem cells (rTDSCs) via the Wnt5a-RhoA pathway. *J Cell Biochem*. 2012; 113(10): 3133–3142, doi: [10.1002/jcb.24190](https://doi.org/10.1002/jcb.24190), indexed in Pubmed: [22615126](https://pubmed.ncbi.nlm.nih.gov/22615126/).
- Yi X, Wu P, Liu J, et al. Candidate kinases for adipogenesis and osteoblastogenesis from human bone marrow mesenchymal stem cells. *Mol Omics*. 2021; 17(5): 790–795, doi: [10.1039/d1mo00160d](https://doi.org/10.1039/d1mo00160d), indexed in Pubmed: [34318850](https://pubmed.ncbi.nlm.nih.gov/34318850/).

25. Anders S, Huber W. Differential expression analysis for sequence count data. *Genome Biol.* 2010; 11(10): R106, doi: [10.1186/gb-2010-11-10-r106](https://doi.org/10.1186/gb-2010-11-10-r106), indexed in Pubmed: [20979621](https://pubmed.ncbi.nlm.nih.gov/20979621/).
26. Anders S, Pyl PT, Huber W. HTSeq-a Python framework to work with high-throughput sequencing data. *Bioinformatics.* 2015; 31(2): 166–169, doi: [10.1186/gb-2010-11-10-r106](https://doi.org/10.1186/gb-2010-11-10-r106), indexed in Pubmed: [25260700](https://pubmed.ncbi.nlm.nih.gov/25260700/).
27. Livak KJ, Schmittgen TD. Analysis of relative gene expression data using real-time quantitative PCR and the 2<sup>(-Delta Delta C(T))</sup> Method. *Methods.* 2001; 25(4): 402–408, doi: [10.1006/meth.2001.1262](https://doi.org/10.1006/meth.2001.1262), indexed in Pubmed: [11846609](https://pubmed.ncbi.nlm.nih.gov/11846609/).
28. Ansaloni S, Selkes N, Snyder J, et al. A streamlined sub-cloning procedure to transfer shRNA from a pSM2 vector to a pGIPZ lentiviral vector. *J RNAi Gene Silencing.* 2010; 6(2): 411–415, indexed in Pubmed: [21139985](https://pubmed.ncbi.nlm.nih.gov/21139985/).
29. Gonçalves MA, Janssen JM, Holkers M, et al. Rapid and sensitive lentivirus vector-based conditional gene expression assay to monitor and quantify cell fusion activity. *PLoS One.* 2010; 5(6): e10954, doi: [10.1371/journal.pone.0010954](https://doi.org/10.1371/journal.pone.0010954), indexed in Pubmed: [20532169](https://pubmed.ncbi.nlm.nih.gov/20532169/).
30. Assis-Ribas T, Forni MF, Winnischofer SM, et al. Extracellular matrix dynamics during mesenchymal stem cells differentiation. *Dev Biol.* 2018; 437(2): 63–74, doi: [10.1016/j.ydbio.2018.03.002](https://doi.org/10.1016/j.ydbio.2018.03.002), indexed in Pubmed: [29544769](https://pubmed.ncbi.nlm.nih.gov/29544769/).
31. Wang Z, Chai C, Wang R, et al. Single-cell transcriptome atlas of human mesenchymal stem cells exploring cellular heterogeneity. *Clin Transl Med.* 2021; 11(12): e650, doi: [10.1002/ctm2.650](https://doi.org/10.1002/ctm2.650), indexed in Pubmed: [34965030](https://pubmed.ncbi.nlm.nih.gov/34965030/).
32. Frith J, Genever P. Transcriptional control of mesenchymal stem cell differentiation. *Transfus Med Hemother.* 2008; 35(3): 216–227, doi: [10.1159/000127448](https://doi.org/10.1159/000127448), indexed in Pubmed: [21547119](https://pubmed.ncbi.nlm.nih.gov/21547119/).
33. van Herpen NA, Schrauwen-Hinderling VB. Lipid accumulation in non-adipose tissue and lipotoxicity. *Physiol Behav.* 2008; 94(2): 231–241, doi: [10.1016/j.physbeh.2007.11.049](https://doi.org/10.1016/j.physbeh.2007.11.049), indexed in Pubmed: [18222498](https://pubmed.ncbi.nlm.nih.gov/18222498/).
34. Singh R, Kaushik S, Wang Y, et al. Autophagy regulates lipid metabolism. *Nature.* 2009; 458(7242): 1131–1135, doi: [10.1038/nature07976](https://doi.org/10.1038/nature07976), indexed in Pubmed: [19339967](https://pubmed.ncbi.nlm.nih.gov/19339967/).
35. Hirsch J, Batchelor B. Adipose tissue cellularity in human obesity. *Clin Endocrinol Metab.* 1976; 5(2): 299–311, doi: [10.1016/s0300-595x\(76\)80023-0](https://doi.org/10.1016/s0300-595x(76)80023-0), indexed in Pubmed: [1085232](https://pubmed.ncbi.nlm.nih.gov/1085232/).
36. Abu-Elheiga L, Matzuk MM, Abo-Hashema KA, et al. Continuous fatty acid oxidation and reduced fat storage in mice lacking acetyl-CoA carboxylase 2. *Science.* 2001; 291(5513): 2613–2616, doi: [10.1126/science.1056843](https://doi.org/10.1126/science.1056843), indexed in Pubmed: [11283375](https://pubmed.ncbi.nlm.nih.gov/11283375/).
37. Abu-Elheiga L, Brinkley WR, Zhong L, et al. The subcellular localization of acetyl-CoA carboxylase 2. *Proc Natl Acad Sci U S A.* 2000; 97(4): 1444–1449, doi: [10.1073/pnas.97.4.1444](https://doi.org/10.1073/pnas.97.4.1444), indexed in Pubmed: [10677481](https://pubmed.ncbi.nlm.nih.gov/10677481/).
38. Soupene E, Kuypers FA. Mammalian long-chain acyl-CoA synthetases. *Exp Biol Med (Maywood).* 2008; 233(5): 507–521, doi: [10.3181/0710-MR-287](https://doi.org/10.3181/0710-MR-287), indexed in Pubmed: [18375835](https://pubmed.ncbi.nlm.nih.gov/18375835/).
39. Sirwi A, Hussain MM. Lipid transfer proteins in the assembly of apoB-containing lipoproteins. *J Lipid Res.* 2018; 59(7): 1094–1102, doi: [10.1194/jlr.R083451](https://doi.org/10.1194/jlr.R083451), indexed in Pubmed: [29650752](https://pubmed.ncbi.nlm.nih.gov/29650752/).
40. Ohsaki Y, Cheng J, Suzuki M, et al. Lipid droplets are arrested in the ER membrane by tight binding of lipidated apolipoprotein B-100. *J Cell Sci.* 2008; 121(Pt 14): 2415–2422, doi: [10.1242/jcs.025452](https://doi.org/10.1242/jcs.025452), indexed in Pubmed: [18577578](https://pubmed.ncbi.nlm.nih.gov/18577578/).
41. Suzuki M, Otsuka T, Ohsaki Y, et al. Derlin-1 and UBXD8 are engaged in dislocation and degradation of lipidated ApoB-100 at lipid droplets. *Mol Biol Cell.* 2012; 23(5): 800–810, doi: [10.1091/mbc.E11-11-0950](https://doi.org/10.1091/mbc.E11-11-0950), indexed in Pubmed: [22238364](https://pubmed.ncbi.nlm.nih.gov/22238364/).
42. Contois JH, McConnell JP, Sethi AA, et al. AACC lipoproteins and vascular diseases division working group on best practices. Apolipoprotein B and cardiovascular disease risk: position statement from the AACC Lipoproteins and Vascular Diseases Division Working Group on Best Practices. *Clin Chem.* 2009; 55(3): 407–419, doi: [10.1373/clinchem.2008.118356](https://doi.org/10.1373/clinchem.2008.118356), indexed in Pubmed: [19168552](https://pubmed.ncbi.nlm.nih.gov/19168552/).
43. Barbier CE, Lind L, Ahlström H, et al. Apolipoprotein B/A-I ratio related to visceral but not to subcutaneous adipose tissue in elderly Swedes. *Atherosclerosis.* 2010; 211(2): 656–659, doi: [10.1016/j.atherosclerosis.2010.03.022](https://doi.org/10.1016/j.atherosclerosis.2010.03.022), indexed in Pubmed: [20382384](https://pubmed.ncbi.nlm.nih.gov/20382384/).
44. Lee Yh, Choi SH, Lee KW, et al. Apolipoprotein B/A1 ratio is associated with free androgen index and visceral adiposity and may be an indicator of metabolic syndrome in male children and adolescents. *Clin Endocrinol (Oxf).* 2011; 74(5): 579–586, doi: [10.1111/j.1365-2265.2010.03953.x](https://doi.org/10.1111/j.1365-2265.2010.03953.x), indexed in Pubmed: [21138461](https://pubmed.ncbi.nlm.nih.gov/21138461/).
45. Pelletier-Beaumont E, Arsenault BJ, Almérás N, et al. Normalization of visceral adiposity is required to normalize plasma apolipoprotein B levels in response to a healthy eating/physical activity lifestyle modification program in visceral obese men. *Atherosclerosis.* 2012; 221(2): 577–582, doi: [10.1016/j.atherosclerosis.2012.01.023](https://doi.org/10.1016/j.atherosclerosis.2012.01.023), indexed in Pubmed: [22321874](https://pubmed.ncbi.nlm.nih.gov/22321874/).
46. Tanoli T, Yue P, Yablonskiy D, et al. Fatty liver in familial hypobetalipoproteinemia: roles of the APOB defects, intra-abdominal adipose tissue, and insulin sensitivity. *J Lipid Res.* 2004; 45(5): 941–947, doi: [10.1194/jlr.M300508-JLR200](https://doi.org/10.1194/jlr.M300508-JLR200), indexed in Pubmed: [14967820](https://pubmed.ncbi.nlm.nih.gov/14967820/).
47. Semenkovich CF. Insulin resistance and atherosclerosis. *J Clin Invest.* 2006; 116(7): 1813–1822, doi: [10.1172/JCI29024](https://doi.org/10.1172/JCI29024), indexed in Pubmed: [16823479](https://pubmed.ncbi.nlm.nih.gov/16823479/).
48. Du T, Zhang J, Yuan G, et al. Nontraditional risk factors for cardiovascular disease and visceral adiposity index among different body size phenotypes. *Nutr Metab Cardiovasc Dis.* 2015; 25(1): 100–107, doi: [10.1016/j.numecd.2014.07.006](https://doi.org/10.1016/j.numecd.2014.07.006), indexed in Pubmed: [25159728](https://pubmed.ncbi.nlm.nih.gov/25159728/).
49. Lamantia V, Bissonnette S, Wassef H, et al. ApoB-lipoproteins and dysfunctional white adipose tissue: Relation to risk factors for type 2 diabetes in humans. *J Clin Lipidol.* 2017; 11(1): 34–45.e2, doi: [10.1016/j.jacl.2016.09.013](https://doi.org/10.1016/j.jacl.2016.09.013), indexed in Pubmed: [28391908](https://pubmed.ncbi.nlm.nih.gov/28391908/).
50. Capece D, D'Andrea D, Begalli F, et al. Enhanced triacylglycerol catabolism by carboxylesterase 1 promotes aggressive colorectal carcinoma. *J Clin Invest.* 2021; 131(11), doi: [10.1172/JCI137845](https://doi.org/10.1172/JCI137845), indexed in Pubmed: [33878036](https://pubmed.ncbi.nlm.nih.gov/33878036/).
51. Ito M, Nagasawa M, Hara T, et al. Differential roles of CIDEA and CIDEC in insulin-induced anti-apoptosis and lipid droplet formation in human adipocytes. *J Lipid Res.* 2010; 51(7): 1676–1684, doi: [10.1194/jlr.M002147](https://doi.org/10.1194/jlr.M002147), indexed in Pubmed: [20154362](https://pubmed.ncbi.nlm.nih.gov/20154362/).
52. Zandbergen F, Mandard S, Escher P, et al. The G0/G1 switch gene 2 is a novel PPAR target gene. *Biochem J.* 2005; 392(Pt 2): 313–324, doi: [10.1042/BJ20050636](https://doi.org/10.1042/BJ20050636), indexed in Pubmed: [16086669](https://pubmed.ncbi.nlm.nih.gov/16086669/).
53. Yang X, Lu X, Lombard M, et al. The G(0)/G(1) switch gene 2 regulates adipose lipolysis through association with adipose triglyceride lipase. *Cell Metab.* 2010; 11(3): 194–205, doi: [10.1016/j.cmet.2010.02.003](https://doi.org/10.1016/j.cmet.2010.02.003), indexed in Pubmed: [20197052](https://pubmed.ncbi.nlm.nih.gov/20197052/).
54. Baburski AZ, Sokanovic SJ, Bjelic MM, et al. Circadian rhythm of the Leydig cells endocrine function is attenuated

- during aging. *Exp Gerontol.* 2016; 73: 5–13, doi: [10.1016/j.exger.2015.11.002](https://doi.org/10.1016/j.exger.2015.11.002), indexed in Pubmed: 26547053.
55. Cole NB, Murphy DD, Grider T, et al. Lipid droplet binding and oligomerization properties of the Parkinson's disease protein alpha-synuclein. *J Biol Chem.* 2002; 277(8): 6344–6352, doi: [10.1074/jbc.M108414200](https://doi.org/10.1074/jbc.M108414200), indexed in Pubmed: 11744721.
  56. Ohsaki Y, Cheng J, Fujita A, et al. Cytoplasmic lipid droplets are sites of convergence of proteasomal and autophagic degradation of apolipoprotein B. *Mol Biol Cell.* 2006; 17(6): 2674–2683, doi: [10.1091/mbc.e05-07-0659](https://doi.org/10.1091/mbc.e05-07-0659), indexed in Pubmed: 16597703.
  57. Zhang H, Wang Y, Li J, et al. Proteome of skeletal muscle lipid droplet reveals association with mitochondria and apolipoprotein a-I. *J Proteome Res.* 2011; 10(10): 4757–4768, doi: [10.1021/pr200553c](https://doi.org/10.1021/pr200553c), indexed in Pubmed: 21870882.
  58. Zehmer JK, Bartz R, Bisel B, et al. Targeting sequences of UBXD8 and AAM-B reveal that the ER has a direct role in the emergence and regression of lipid droplets. *J Cell Sci.* 2009; 122(Pt 20): 3694–3702, doi: [10.1242/jcs.054700](https://doi.org/10.1242/jcs.054700), indexed in Pubmed: 19773358.
  59. Lyu Y, Su X, Deng J, et al. Defective differentiation of adipose precursor cells from lipodystrophic mice lacking perilipin 1. *PLoS One.* 2015; 10(2): e0117536, doi: [10.1371/journal.pone.0117536](https://doi.org/10.1371/journal.pone.0117536), indexed in Pubmed: 25695774.
  60. Čopič A, Antoine-Bally S, Giménez-Andrés M, et al. A giant amphipathic helix from a perilipin that is adapted for coating lipid droplets. *Nat Commun.* 2018; 9(1): 1332, doi: [10.1038/s41467-018-03717-8](https://doi.org/10.1038/s41467-018-03717-8), indexed in Pubmed: 29626194.
  61. Umlauf E, Csaszar E, Moertelmaier M, et al. Association of stomatin with lipid bodies. *J Biol Chem.* 2004; 279(22): 23699–23709, doi: [10.1074/jbc.M310546200](https://doi.org/10.1074/jbc.M310546200), indexed in Pubmed: 15024010.
  62. Justesen J, Stenderup K, Ebbesen EN, et al. Adipocyte tissue volume in bone marrow is increased with aging and in patients with osteoporosis. *Biogerontology.* 2001; 2(3): 165–171, doi: [10.1023/a:1011513223894](https://doi.org/10.1023/a:1011513223894), indexed in Pubmed: 11708718.
  63. Verma S, Rajaratnam JH, Denton J, et al. Adipocytic proportion of bone marrow is inversely related to bone formation in osteoporosis. *J Clin Pathol.* 2002; 55(9): 693–698, doi: [10.1136/jcp.55.9.693](https://doi.org/10.1136/jcp.55.9.693), indexed in Pubmed: 12195001.
  64. Song L, Tuan RS. Transdifferentiation potential of human mesenchymal stem cells derived from bone marrow. *FASEB J.* 2004; 18(9): 980–982, doi: [10.1096/fj.03-1100fje](https://doi.org/10.1096/fj.03-1100fje), indexed in Pubmed: 15084518.
  65. Alexanian AR. Epigenetic modulators promote mesenchymal stem cell phenotype switches. *Int J Biochem Cell Biol.* 2015; 64: 190–194, doi: [10.1016/j.biocel.2015.04.010](https://doi.org/10.1016/j.biocel.2015.04.010), indexed in Pubmed: 25936755.
  66. Naskar S, Kumaran V, Markandeya YS, et al. Neurogenesis-on-Chip: Electric field modulated transdifferentiation of human mesenchymal stem cell and mouse muscle precursor cell coculture. *Biomaterials.* 2020; 226: 119522, doi: [10.1016/j.biomaterials.2019.119522](https://doi.org/10.1016/j.biomaterials.2019.119522), indexed in Pubmed: 31669894.
  67. Zhang C, Li L, Jiang Y, et al. Space microgravity drives transdifferentiation of human bone marrow-derived mesenchymal stem cells from osteogenesis to adipogenesis. *FASEB J.* 2018; 32(8): 4444–4458, doi: [10.1096/fj.201700208RRR](https://doi.org/10.1096/fj.201700208RRR), indexed in Pubmed: 29533735.
  68. Costa V, Carina V, Raimondi L, et al. MiR-33a controls hMSCS osteoblast commitment modulating the Yap/Taz expression through EGFR signaling regulation. *Cells.* 2019; 8(12), doi: [10.3390/cells8121495](https://doi.org/10.3390/cells8121495), indexed in Pubmed: 31771093.
  69. Zhang Y, Ling L, Ajay D/O Ajayakumar A, et al. FGFR2 accommodates osteogenic cell fate determination in human mesenchymal stem cells. *Gene.* 2022 [Epub ahead of print]; 818: 146199, doi: [10.1016/j.gene.2022.146199](https://doi.org/10.1016/j.gene.2022.146199), indexed in Pubmed: 35093449.
  70. Knani L, Bartolini D, Kechiche S, et al. Melatonin prevents cadmium-induced bone damage: First evidence on an improved osteogenic/adipogenic differentiation balance of mesenchymal stem cells as underlying mechanism. *J Pineal Res.* 2019; 67(3): e12597, doi: [10.1111/jpi.12597](https://doi.org/10.1111/jpi.12597), indexed in Pubmed: 31340072.
  71. Li H, Zhou W, Sun S, et al. Microfibrillar-associated protein 5 regulates osteogenic differentiation by modulating the Wnt/ $\beta$ -catenin and AMPK signaling pathways. *Mol Med.* 2021; 27(1): 153, doi: [10.1186/s10020-021-00413-0](https://doi.org/10.1186/s10020-021-00413-0), indexed in Pubmed: 34865619.

*Submitted: 15 November, 2021*

*Accepted after reviews: 9 February, 2022*

*Available as AoP: 25 February, 2022*